

Article

Exciton Spectroscopy of Spatially Separated Electrons and Holes in the Dielectric Quantum Dots

Sergey I. Pokutnyi ^{1,*}, Yuri N. Kulchin ², Vladimir P. Dzyuba ² and David B. Hayrapetyan ³

¹ Department of Theoretical Physics, Chuiko Institute of Surface Chemistry of National Academy of Sciences of Ukraine, 17 General Naumov Str., UA 03164 Kyiv, Ukraine

² Institute of Automation and Control Processes Far East Branch Russian Academy of Sciences, 5 Radio Str., Vladivostok 690042, Russia; kulchin@iacp.dvo.ru (Y.N.K.); vdzyuba@iacp.dvo.ru (V.P.D.)

³ Russian-Armenian University, 123 H. Emin, Yerevan 0051, Armenia; dhayrap82@gmail.com

* Correspondence: Pokutnyi_Sergey@inbox.ru

Received: 26 February 2018; Accepted: 25 March 2018; Published: 27 March 2018



Abstract: It is shown that in the potential energy of an exciton of spatially separated electrons and holes (hole moves in the amount of quantum dots (QDs), and the electron is localized on a spherical surface section (QD—dielectric matrix)) taking into account centrifugal energy gives rise band of the quasi-stationary surface exciton states that with the increase of the radius of QD becomes stationary state. The mechanisms of formation of the spectra of interband and intraband absorption (emission) of light in nanosystems containing aluminum oxide QDs, placed in the matrix of vacuum oil, are presented. It is shown that the electron transitions in the area of the surface exciton states cause significant absorption in the visible and near infrared wavelengths, and cause the experimentally observed significant blurring of the absorption edge.

Keywords: exciton of spatially separated electrons and holes; quasi-stationary and stationary states; quantum dots

1. Introduction

Investigation of quasi-zero nanosystems consisting of semiconductor (dielectric) spherical form quantum dots (QDs) with the radii $a = 1\text{--}10$ nm, containing CdS, ZnSe and aluminum oxide in their volume, which were grown in the transparent dielectric matrix, such as borosilicate glass, vacuum and immersion oils, has received increased attention due to their unique photoluminescent properties and the ability of the efficiently emitting light in the visible or near infrared regions at room temperature [1–4]. Such linear dimensions a of QD are comparable with the de Broglie wavelength of the electron and hole or/and their Bohr radii. The optical properties of quasi-zero nanosystems are largely determined by the energy spectrum of the spatially separated electron-hole pairs (excitons) [5–8].

There are many works devoted to the investigation of different physical characteristics of quantum dots with different geometries. For example, in [9], the authors study intrinsic defect centers such as oxygen and zinc vacancies in ZnO nanocrystals. The core-shell model established from optical emission and electron paramagnetic resonance suggests distinguished electronic states in the band gap belonging to negatively charged Zn vacancies and positively charged oxygen vacancies. In [10] the authors report the formation of highly luminescent organic capped colloidal cadmium sulfide (CdS) nanoparticles having the highest photoluminescence quantum yield of 69% in solutions and 34% in neat thin films in the near-infrared range.

The synthesis of ZnO nanoparticles by solid state and hydrolysis methods based on the conventional precipitation is reported in [11]. Novel ZnS quantum dots and ZnS quantum flakes were

successfully prepared with graphene nanosheets as a special template, and two unique heterostructures of ZnS/GNs were also obtained in [12]. The synthesis of ZnO 3.4 nm diameter spherical nanoparticles for the implementation them as an electron injection layer in large-area emitters leads to efficient solution-based devices is reported in [13].

In the experimental work [1] it is found that the non-equilibrium electrons generated by the interband excitation of CdS QDs with radii $a = (1.5\text{--}30)$ nm, have a finite probability of overcoming the potential barrier and penetration into the matrix of borosilicate glass, where the QD is immersed (wherein the hole moves in the QD volume).

In [5,6] it is developed the theory of the exciton from spatially separated electrons and holes (the hole is within the volume of the semiconductor (dielectric) QD, and the electron is localized over the spherical surface boundary of (QD/matrix)). The effect of a significant increase of the binding energy of an exciton is revealed in nanosystem containing semiconductor (CdS, CdSe, ZnSe) and aluminum oxide (almost by two orders) dielectric QD in comparison with the binding energy of an exciton in such single crystals materials.

In experimental works [2–4] the nonlinear optical properties and their dependences on the matrix material (vacuum oil) of heterogeneous liquid nanophase composites based on wideband aluminum oxide QD with average radii not exceeding $a = 25$ nm were studied. In [2–4] it is shown that aluminum oxide QDs in such matrix have a wide absorption band in the visible and near-infrared wavelengths.

In [2–4] the nature of the absorption bands in the visible and near infrared regions remains unclear. Therefore, the study of light absorption mechanisms in such nanoheterostructures is an actual problem.

The present work summarizes the theory of excitons from spatially separated electrons and holes (the hole moves in volume QD, and the electron is localized over the spherical surface boundary of (QD/matrix)), developed in [5,6], for the case in which centrifugal energy of the electron is considered in the potential energy of the exciton. It has been shown that considering the centrifugal energy in the potential energy of the exciton leads to the occurrence of the quasi-stationary states in the band of the surface exciton states, which with the increase of QD radius transfers into stationary state. It is established that the light spectrum of the interband absorption (emission) of nanosystems consisting of the energy bands which are formed by the electron between quasi-stationary and stationary states, and intraband absorption spectra—from the bands caused by electron transitions between stationary states.

2. Energy of Ground State Exciton in Nanosystems

Consider the model of quasi-zero-nanosystems: Semiconductor spherical QD with a radius, which contains in its volume semiconductor (dielectric) material with permittivity ε_2 , surrounded by a dielectric matrix with ε_1 permittivity. In the QD volume h hole moves with the effective mass m_h , and e electron with the effective mass $m_e^{(1)}$ is situated in the matrix (r_e and r_h —the distance of electron and hole from the QD center). Let us assume that in QD the valence band has a parabolic form. We also assume that on the spherical surface boundary of QD/matrix infinite high potential barrier exists. Therefore, in the studied model h hole cannot go out from the QD volume, and e electron can not penetrate into the QD volume.

The energy of polarization interaction of the electron and hole $U(r_e, r_h, a)$ with spherical surface boundary of QD/matrix in the case of relative $\varepsilon = (\varepsilon_2/\varepsilon_1) \gg 1$ permittivity can be represented as the algebraic sum of the hole and electron interaction energies with their $V_{hh'}(r_h, a)$, $V_{ee'}(r_e, a)$ and “foreign” $V_{eh'}(r_e, r_h, a)$, $V_{he'}(r_e, r_h, a)$ images, respectively [5]:

$$U(r_e, r_h, a, \varepsilon) = V_{hh'}(r_h, a, \varepsilon) + V_{ee'}(r_e, a, \varepsilon) + V_{eh'}(r_e, r_h, a, \varepsilon) + V_{he'}(r_e, r_h, a, \varepsilon) \quad (1)$$

where

$$V_{hh'}(r_h, a, \varepsilon) = \frac{e^2\beta}{2\varepsilon_2 a} \left(\frac{a^2}{a^2 - r_h^2} + \varepsilon \right) \quad (2)$$

$$V_{ee'}(r_e, a, \epsilon) = -\frac{e^2\beta}{2\epsilon_1 a} \cdot \frac{a^4}{r_e^2(r_e^2 - a^2)} \tag{3}$$

$$V_{he'}(r_e, r_h, a, \epsilon) = \frac{e^2\beta}{2\epsilon_2 a} \cdot \frac{a^2}{r_e |r_h - (a/r_e)^2 r_e|} \tag{4}$$

$$V_{eh'}(r_e, r_h, a, \epsilon) = -\frac{e^2\beta}{2\epsilon_1 a} \cdot \frac{a^2}{r_h |r_e - (a/r_h)^2 r_h|} \tag{5}$$

Here the parameter of the nanosystem $\beta = (\epsilon_2 - \epsilon_1)/(\epsilon_2 + \epsilon_1)$.

For the simplicity, without losing the generality, we will assume that the hole h with the effective mass m_h , is located in the center of the QD (wherein $r_h = 0$), and the e electron with an effective mass $m_e^{(1)}$ is localized in the matrix of the spherical surface QD ($r_e = r$ —the distance of e electron from the QD center). Such assumption is justified, as the ratio of the effective masses of electrons and holes in nanosystem ($(m_e^{(1)}/m_h) \ll 1$). In the observed quasi-zero nanosystems model, in the frame of the above mentioned approximations, as well as in the effective mass approximation and the center of mass of nanosystem, the Hamiltonian of exciton (from spatially separated hole, moving in QD volume, and the electron situated in the dielectric matrix) takes the form:

$$H(r, a) = -\frac{\hbar^2}{2\mu_0} \Delta + V_l(r) + V_{eh}(r) + U(r, a) + E_g \tag{6}$$

where the first member is the operator of exciton’s kinetic energy, ($\mu_0 = m_e^{(1)}m_h/(m_e^{(1)} + m_h)$ —the reduced mass of the exciton from spatially separated electrons and holes), the second describes the centrifugal energy of the exciton

$$V_l(r) = \frac{\hbar^2 L^2}{2\mu_0 r^2} \tag{7}$$

($L^2 = l(l + 1)$, $l = 0, 1, 2$,—orbital quantum number of the electron), E_g —width of semiconductor bandgap with ϵ_2 permittivity. In the Hamiltonian (6), the energy of the Coulomb interaction between the electron and hole is described by the equation [5]:

$$V_{eh}(r) = -\frac{1}{2} \left(\frac{1}{\epsilon_1} + \frac{1}{\epsilon_2} \right) \frac{e^2}{r} = -\frac{e^2}{\tilde{\epsilon} r} \tag{8}$$

Polarization interaction energy (2), (4), (5) of electron and hole with spherical surface boundary of QD/matrix, when $r_h = 0$, takes the form:

$$V_{hh'}(a) = \frac{e^2\beta}{2\epsilon_2 a} \left(1 + \frac{\epsilon_2}{\epsilon_1} \right) \tag{9}$$

$$V_{he'}(a) = \frac{e^2\beta}{2\epsilon_2 a} \tag{10}$$

$$V_{eh'}(a) = -\frac{e^2\beta}{2\epsilon_1 a} \tag{11}$$

Then taking into account (3), (9), (10) and (11), the energy of polarization interaction (3), may be written in the following form:

$$U(r, a) = -\frac{e^2\beta}{2\epsilon_1 a} \cdot \frac{a^4}{r^2(r^2 - a^2)} + \frac{e^2\beta}{\epsilon_2 a} \tag{12}$$

Consideration of interaction energy of hole with its (9) and “foreign” (10) images, as well as the electron with the “foreign” (11) image, leads to the increase of the polarization interaction energy (9) by $(e^2\beta/\epsilon_2a)$, which decreases with the increase of QD radius.

In the nanosystem the Hamiltonian $H(r, a)$ (6) of the exciton from spatially separated electron and hole considering the formulas (7), (8) and (12) takes the following form:

$$H(r, a) = -\frac{\hbar^2}{2\mu_0}\Delta + U_l(r, a) + E_g \tag{13}$$

where effective potential energy of the exciton

$$U_l(r, a) = -\frac{e^2}{\epsilon r} - \frac{e^2\beta}{2\epsilon_1a} \cdot \frac{a^4}{r^2(r^2 - a^2)} + \frac{e^2\beta}{\epsilon_2a} + \frac{\hbar^2L^2}{2\mu_0r^2} \tag{14}$$

with the increase of the QD radius (so that $a \gg a_{ex}$, where $a_{ex} = (\epsilon_2 \hbar^2 / \mu e^2)$ —exciton Bohr radius, $\mu = m_e^{(2)} m_h / (m_e^{(2)} + m_h)$ is the reduced exciton mass and $m_e^{(2)}$ —the effective mass of electron in the semiconductor with permittivity ϵ_2), the spherical surface between boundary of two media goes into the flat boundary surface. Wherein the exciton from the spatially separated electrons and holes (the hole moves in the semiconductor, and the electron is situated in the matrix) becomes two-dimensional. In the Hamiltonian (6) potential energy, describing the motion of the exciton in the nanosystem, containing QD with large radius ($a \gg a_{ex}$) the main contribution is the energy of the Coulomb interaction $V_{eh}(r)$ (8) between electron and hole. Interaction energy between electron and hole with their (9), (11) and “foreign” (11), (10) images gives a much smaller contribution to the potential energy (14) of the Hamiltonian (6). By the first approximation this contribution may be neglected. In the potential energy (14) of the Hamiltonian (6) remains only the energy of the Coulomb interaction (8) between electron and hole. The Schrodinger equation with this Hamiltonian describes a two-dimensional exciton (2D exciton) from spatially separated electron and hole energy spectrum, which takes the form [14]:

$$E_n = -\frac{Ry_{ex}^{2D}}{(n + (1/2))^2}, \quad Ry_{ex}^{2D} = \frac{(\epsilon_1 + \epsilon_2)^2}{4\epsilon_1^2\epsilon_2^2} \cdot \left(\frac{\mu_0}{m_0}\right) Ry_0 \tag{15}$$

where $n = 0, 1, 2, \dots$ —the principal quantum number of exciton, $Ry_0 = 13.606$ eV—the Rydberg constant. Bohr radius of such 2D exciton is described by the following equation:

$$a_{ex}^{2D} = \frac{2\epsilon_1\epsilon_2}{\epsilon_1 + \epsilon_2} \cdot \frac{\hbar^2}{\mu_0e^2} \tag{16}$$

and the binding energy of the ground state of 2D exciton, according to (15), is given by:

$$E_{ex}^{2D} = -4Ry_{ex}^{2D} \tag{17}$$

If $l \neq 0$, the contribution of the centrifugal energy into the effective potential energy $U_l(r, a)$ (14) creates a positive potential barrier, the maximum value of which is the following

$$U^{max}(l, S) \sim L^2S^{-2} \tag{18}$$

for QD with large radius $S \gg 1$ ($S = (a/a_{ex}^{2D})$ —the dimensionless radius of QD). The formation of such barrier means that along with the stationary states $E_{1,l}(S) < 0$ the exciton (from spatially separated electrons and holes), over the spherical surface of the QD, can occur quasi-stationary states of the exciton with energy $E_{1,l}(S) > 0$. With the increase of radius S of QD, starting from the value of S greater than a certain critical radius of $S_c^*(1, l)$, i.e., at

$$S > S_c^*(1, l) \tag{19}$$

first quasi-stationary states should be appeared. At bigger radii of QD

$$S > S_c(1, l) > S_c^*(1, l) \tag{20}$$

they need to pass into stationary states. When $S \geq \tilde{S}_c(1, l) \gg 1$ stationary states passes into two-dimensional exciton state with energy $E_{1,l}(a) = (-E_{ex}^{2D})$ (14), localized on flat surface between two media [5,6], i.e., the energy spectrum $E_{1,l}(S)$ of the stationary states of the exciton energy is bounded from below $(-E_{ex}^{2D})$ (14). The existence of the critical radius $S_c^*(1, l)$ shows that for QD with determined radius S the energy spectrum $E_{1,l}(S)$ of the exciton is bounded above by the maximum value $l^{max}(1, S)$, forming a band of surface states, localized on the surface spherical boundary of (QD/matrix), part of which has a quasi-stationary character. Such band of surface states contains a finite number of levels $(1, l)$, and this band is finished by $(1, l^{max}(l, S))$ level. Radius $S_c^*(1, l)$ corresponds to the highest acceptable value of energy $E_{1,l}^{max}(S)$ of ground state at fixed l . This maximum value of the energy coincides with the $U^{max}(l, S = S_c^*(1, l))$ (15).

Let us define the energy of the ground ($n = 1$) state of the exciton Hamiltonian (10) for arbitrary values of S and l by means of variational method. By making a standard replacement of the radial wave function $R_l(r) = (\chi_l(r)/r)$, the variational function $\chi_l(r)$ will be given as:

$$\begin{aligned} \chi_l(r) &= A_l r(r - a) \exp(-j_l(r - a)/a) \\ A_l &= 2(j_l/S)^{5/2} (a_{ex}^{2D})^{-5/2}, \end{aligned} \tag{21}$$

where $j_l(a)$ —variational parameter. Choosing the wave function $\chi_l(r)$ in the form (21) provides its passage to the limit when $S \rightarrow \infty$, $(j_l/S) \rightarrow const$ in the wave function of electrons localized on the plane surface between two media [15,16]. We write the mean value of the exciton Hamiltonian (10) on the wave functions (18) in the following form:

$$E_{1,l}(a, j_l(a)) = \langle R_l(r) | H(r, a) | R_l(r) \rangle \tag{22}$$

The results of the variational calculation of energy $E_{1,l}(a)$ (22) of the ground state of the exciton in nanosystems containing aluminum oxide QD with average a radius not exceeding 20 nm, are obtained for the nanosystem containing aluminum oxide QD (with permittivity $\epsilon_2 = 10$ and the effective mass of hole $(m_h/m_0) = 6.2$; the value of the effective mass of the electron in the matrix $(m_e^{(1)}/m_0) = 0.537$ [17], situated in the matrix (vacuum oil), which was studied in experimental studies [2–4] (see Figure 1). Figure 1 shows the dependence of $E_{1,l}(a)$ (19) for the states with $l = 0, 1, 2, 3, 4, 5, 6, 7, 8$ with quasi-stationary states spectrum border $E_{1,l}^{max}(a)$. The obtained results (see Figure 1) clearly illustrate the abovementioned qualitative features of considered dependences $E_{1,l}(a)$ (22). The critical radii of QD for $l \leq 8$ have are respectively values:

$$\begin{aligned} a_c^*(1, l)(S_c^*(1, l)) &= 4.9 \text{ nm (13.94); } 6.64 \text{ nm (18.9); } \\ &8.48 \text{ nm (24.12); } 10.22 \text{ nm (29.1); } 11.82 \text{ nm (33.6); } \\ &13.5 \text{ nm (38.4); } 15.2 \text{ nm (43.2); } 16.8 \text{ nm (47.8); } \\ a_c(1, l)(a_c(1, l)) &= 3.1 \text{ nm (8.82); } 5.0 \text{ nm (14.22)} \\ &6.83 \text{ nm (19.43); } 8.63 \text{ nm (24.55); } \\ &10.4 \text{ nm (29.6); } 12.14 \text{ nm (34.5); } \\ &13.84 \text{ nm (39.4); } 15.5 \text{ nm (44.1); } 17.16 \text{ nm (48.8)} \end{aligned} \tag{23}$$

In nanosystems with the increase of radius a of QD, starting from the value not exceeding a certain critical radius of QD $a_c^*(1, l)$ at

$$a_c^*(1, l) \leq a \leq a_c(1, l) \tag{24}$$

quasi-stationary states of the exciton firstly appear (see Figure 1). For instance, the smallest radius $a_c^*(1, l)$ of QD in which case quasi-stationary states of the exciton appear (in the state $(1, l = 1)$)

according to (20) is equaled to $a_c^*(1, 1) \cong 4.9$ nm, whereas the largest radius of QD $a_c^*(1, l)$, at which the quasi-stationary state exciton occurs (in the state $(1, l = 8)$ is equaled to $a_c^*(1, l = 8) \cong 16.8$ nm).

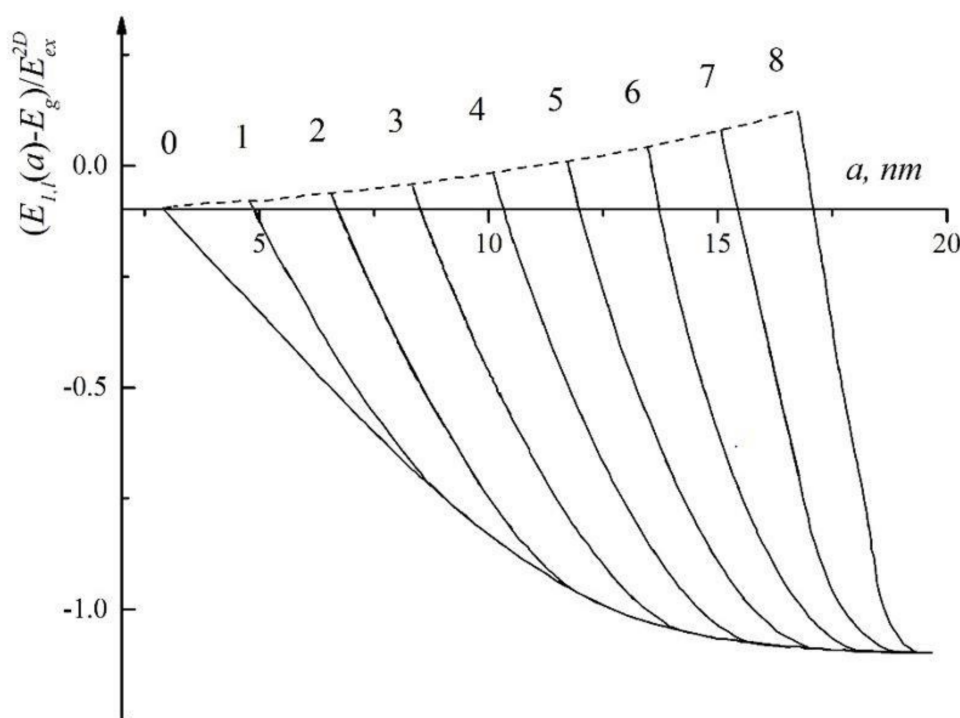


Figure 1. The dependence of the energy spectrum $(E_{1,l}(a) - E_g)$ of the exciton (from spatially separated electrons and holes) in the states $(n = 1, l = 0, 1, 2, 3, 4, 5, 6, 7, 8)$ (where n and l —the principal and orbital quantum numbers of the electron) (solid line) on the a radius of the aluminum oxide QD, situated in the dielectric matrix (vacuum oil). The numbers at the curves indicate the value of l . The dashed lines indicate the boundaries of the spectrum of quasi-stationary states $E_{1,l}^{max}(a)$ of the exciton. Here E_g —bandgap of the aluminum oxide QD, $E_{ex}^{2D} = 2.5038$ eV—the binding energy of the ground state of the two-dimensional exciton (from spatially separated electrons and holes).

In the range of values of QD radii

$$a_c(1, l) \leq a \leq \tilde{a}_c(1, l) \tag{25}$$

(at $a \geq \tilde{a}_c(1, l) = 19.1$ nm quasi-stationary states $(1, l)$ of the exciton goes into the two-dimensional exciton state (12) localized on a flat surface bounding two media [5,6]), and the quasi-stationary state goes into the exciton stationary states (see Figure 1). The smallest radius of QD $a_c(1, l)$ at which the exciton stationary states appear (in the state $(1, l = 0)$, according to (20) is equaled to $a_c(1, 0) \cong 3.1$ nm [5,6], wherein the largest radius of QD $a_c(1, l)$ (in exciton state $(1, l = 8)$) $a_c(1, l = 8) \cong 17.16$ nm. In nanosystem the stationary states of the exciton (from spatially separated electrons and holes) are located in the bandgap of aluminum oxide QD (below the bottom of the conduction band E_s of aluminum oxide QD (see Figure 2, area 1)). They are limited below by level $E_{ex}^{2D} \cong 2.504$ eV (14), which is equal to the binding energy of the ground state of two-dimensional exciton (from spatially separated electrons and holes). Quasi-stationary states of the exciton are in the conduction band E_s (above the bottom of the conduction band E_s of aluminum oxide QD (see Figure 2, area 2). They are limited to the top by the border of the spectrum $E_{1,l}^{max}(a)$ of quasi-stationary states. The magnitude of $E_{1,l}^{max}(a)$ takes a maximum value in the state $(1, l = 8)$, wherein the $E_{1,l=8}^{max}(a = a_c^*(1, l = 8) \cong 0.21 E_{ex}^{2D} \cong 0.526$ eV) (see Figure 1). In the nanosystem hole moves in the

valence band E_v of QD, and the electron is in the quasi-stationary and stationary states (in areas 1 and 2 of the conduction band and the band gap of QD, see Figure 2).

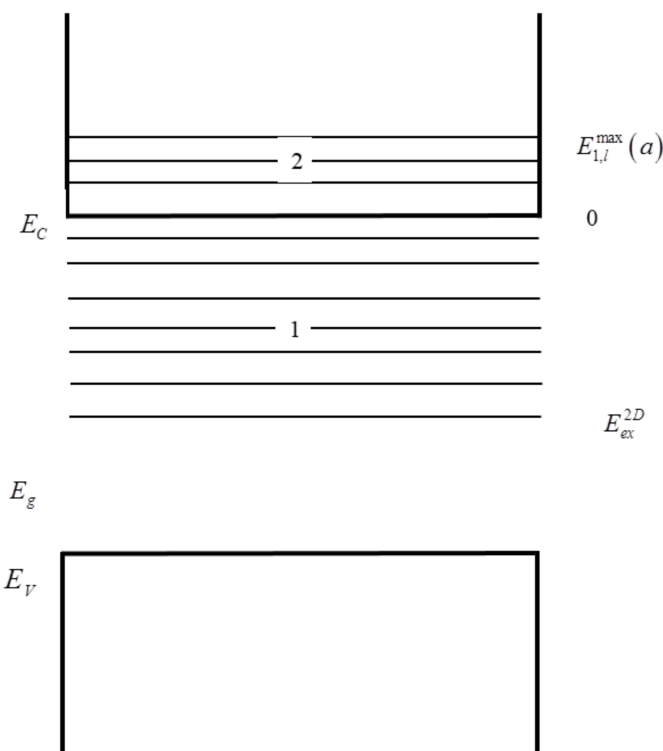


Figure 2. Schematic representation of the energy levels $E_{1,l}(a)$ of the exciton (from spatially separated electron and hole) in the state ($n = 1, l \leq 8$) in the nanosystem consisting of Al₂O₃ QD with a radius situated the dielectric matrix (vacuum oil). The stationary states of the exciton (area 1) are located in the bandgap of Al₂O₃ QD (below the bottom of the conduction band E_s of Al₂O₃ QD). They are bounded below by level E_{ex}^{2D} , which is the binding energy of the ground state of the exciton (from spatially separated electrons and holes) in the nanosystems. Quasi-stationary states of the exciton (area 2) are in the E_s conduction band of Al₂O₃ QD (above the bottom of the conduction band E_s). They are limited to the top boundary of the spectrum of quasi-stationary states $E_{1,l}^{max}(a)$ (see Figure 1). In this case, the hole moves in the valence band of QD, and the electron is located on energy levels (in area 1 and 2).

Such high quasi-stationary states could be significant in the processes of scattering of electrons on the QD with sufficient large radius $a \cong a_c^*(1, 8) \cong 16.8$ nm and may lead to strong suppression of the electron mobility in dielectric matrices. The electron trapping on the quasi-stationary states, herewith it is possible also without changing the total energy.

Thus, for aluminum oxide QD, which radius is in the interval (25), the energy spectrum $E_{1,l}(a)$ of the exciton is limited above by the maximum value of the orbital quantum number $l^{max} = 8$, forming surface states band. Such band of the surface states of the exciton (from spatially separated electron and hole) consists of stationary and quasi-stationary states and has a finite number of levels ($1, l$), is equal to nine.

Obtained results allow us to follow the transition from the exciton states localized on the surface of a spherical QD, to the states of the exciton localized on the boundary plane surface. For QD with large radius S (in the limit of $S \rightarrow \infty$) not only arbitrary values of l , but also (l/S) , which within $(S, l \rightarrow \infty)$ define the finite quasimomentum $p = \hbar k_{||} = (\hbar l/a)$ of free movement of the electron parallel to the boundary surface, become permitted. As a result, the expression $E_{1,l}(a)$ (22) proceeds

into the spectrum of exciton states localized on the boundary plane surface, which in the dimensional units has a following form

$$E_{1,l}(k_{\parallel}) = -E_{ex}^{2D} + (\hbar^2 k_{\parallel}^2) / 2\mu_0 \quad (26)$$

Thus, all surface states become stationary, as in the case of specified passage to the limit potential barrier (14) becomes infinitely wide, and its height (18) $U^{max}(l, S) \rightarrow (L^2/S^2) = (\hbar^2 k_{\parallel}^2) / 2\mu_0$ (in the dimensional units) defines the kinetic energy of the “free” motion of the electron along the plane of the media boundary.

The more elementary method to detect and study of observed exciton states in nanosystems consisting of aluminum oxide with an average radius of a (25) placed in the matrix (vacuum oil) [2–4], can be investigated the interband, which is formed by the electron transitions in the surface exciton states band between the quasi-stationary states, located in the conductivity band E_s of QD and stationary states, being in the band gap of the QD (see Figure 2)) and intraband (which is caused by the electron transitions between the stationary states) of light absorption. Such transitions with a change in the orbital quantum number ($l' = l \pm 1$) per unit are allowed by the selection rules. The photon energy for such transitions

$$\Delta E_l^{l+1}(a) = E_{1,l+1}(a) - E_{1,l}(a) \quad (27)$$

(where l is takes values from 0 to 8).

Consider the qualitative picture of the appearance of transition states in nanosystem (see Figures 1 and 2 and Table 1). Starting from the radius of aluminum oxide QD $a \geq a_c^*(1, 1) \cong 4.9$ nm in the range of QD radii:

$$a_c^*(1, 1) \leq a < (a_c^*(1, 2) \cong 6.64 \text{ nm}) \quad (28)$$

interband transition occurs between states of (1, 1) and (1, 0) photons with energies in the range of

$$248 \text{ meV} < \Delta E_0^1(a) \leq 551 \text{ meV} \quad (29)$$

Table 1. Energy transitions $\Delta E_{l-1}^l(a)$ (expressed by meV), in which the orbital quantum number l changes by one (wherein l takes values from 1 to 8) between quasi-stationary and stationary states of the exciton (from the spatially separated electrons and holes) (see Figure 1), appearing in the nanosystem containing aluminum oxide QD with a radius (expressed by nm), situated in the dielectric matrix (vacuum oil).

a (nm)	$\Delta E_0^1(a)$ (meV)	$\Delta E_1^2(a)$ (meV)	$\Delta E_2^3(a)$ (meV)	$\Delta E_3^4(a)$ (meV)	$\Delta E_4^5(a)$ (meV)	$\Delta E_5^6(a)$ (meV)	$\Delta E_6^7(a)$ (meV)	$\Delta E_7^8(a)$ (meV)
5.2	501							
5.3	426							
5.6	401							
5.8	351							
6.0	325							
6.5	250							
6.9	200	826						
7.2	180	801						
7.5	150	751						
8.0	75	676						
8.6	24	570	1150					
9.0	0	451	926					
9.5	0	325	851					
10	0	225	751					
10.3	0	201	701	1172				

Table 1. Cont.

a (nm)	$\Delta E_0^1(a)$ (meV)	$\Delta E_1^2(a)$ (meV)	$\Delta E_2^3(a)$ (meV)	$\Delta E_3^4(a)$ (meV)	$\Delta E_4^5(a)$ (meV)	$\Delta E_5^6(a)$ (meV)	$\Delta E_6^7(a)$ (meV)	$\Delta E_7^8(a)$ (meV)
11	0	75	576	976				
11.9	0	0	350	750	1192			
12.5	0	0	225	651	1080			
13	0	0	124	502	976			
13.6	0	0	52	388	851	1352		
14	0	0	0	275	626	1302		
15.2	0	0	0	63	376	1001	1480	
16	0	0	0	0	150	501	1281	
16.9	0	0	0	0	0	224	628	2000
17.5	0	0	0	0	0	63	300	1552
18	0	0	0	0	0	0	150	1052
18.5	0	0	0	0	0	0	34	401
18.8	0	0	0	0	0	0	0	72
19.1	0	0	0	0	0	0	0	0

With the increase of the radius a of QD in the range of radii a

$$a_c^*(1, 2) \leq a < (a_c^*(1, 3) \cong 8.48 \text{ nm}) \quad (30)$$

there are two interband transitions: The transition between the states (1, 1) and (1, 0) with photon energies in the range of

$$248 \text{ meV} \leq \Delta E_0^1(a) < 25 \text{ meV} \quad (31)$$

and transition between states (1, 2) and (1, 1) in the range of QD radii

$$a_c^*(1, 2) \leq a < (a_c(1, 2) \cong 6.83 \text{ nm}) \quad (32)$$

with the energy of the quantum

$$\Delta E_1^2(a) \cong 826 \text{ meV} \quad (33)$$

and in the range of QD radii

$$a_c(1, 2) \leq a < a_c^*(1, 3) \quad (34)$$

such transition is intraband with energies of the quantum in the range of

$$526 \text{ meV} < \Delta E_1^2(a) \leq 826 \text{ meV} \quad (35)$$

in the range of QD radii

$$a_c^*(1, 3) \leq a < (a_c^*(1, 4) \cong 10.22 \text{ nm}) \quad (36)$$

interband transition between (1, 3) and (1, 2) is added to two transitions which occur in the range of QD a radii (30), which range in radii of QD

$$a_c^*(1, 3) \leq a < (a_c(1, 3) \cong 8.63 \text{ nm}) \quad (37)$$

will be interband with photon energy

$$\Delta E_2^3(a) \cong 1.0 \text{ meV} \quad (38)$$

in the range of QD radii

$$a_c(1, 3) \leq a < a_c^*(1, 4) \quad (39)$$

such transition is intraband with photons energies

$$0.694 \text{ meV} < \Delta E_2^3(a) \leq 1.0 \text{ meV}$$

In the range of a radii of QD (36) intraband transition between states (1, 2) and (1, 1) will be observed with photon energies in the range of

$$175 \text{ meV} < \Delta E_1^2(a) \leq 526 \text{ meV} \quad (40)$$

Intraband transitions between the states (1, 1) and (1, 0) disappears when $a \cong 9.1$ nm. In the range of radii of QD

$$a_c^*(1, 4) \leq a < (a_c^*(1, 5) \cong 11.82 \text{ nm}) \quad (41)$$

three transitions exist: intraband transitions between the states (1, 2) and (1, 1), which, with energy not exceeding (188 meV), disappears when $a \cong 11.6$ nm, and intraband transitions between the states (1, 3) and (1, 2) with photon energies

$$351 \text{ meV} \leq \Delta E_2^3(a) \leq 701 \text{ meV} \quad (42)$$

Arising new transition between (1, 4) and (1, 3) states in the range of a radii of QD

$$a_c^*(1, 4) \leq a < (a_c(1, 5) \cong 10.4 \text{ nm}) \quad (43)$$

is interband with a photon energy

$$\Delta E_3^4(a) \cong 1.108 \text{ eV} \quad (44)$$

in the range of radii

$$a_c(1, 4) \leq a < a_c^*(1, 5) \quad (45)$$

such transition will be intraband with photons energies

$$0.801 \text{ eV} < \Delta E_3^4(a) \leq 1.108 \text{ eV} \quad (46)$$

In the range of a

$$a_c^*(1, 5) \leq a < (a_c^*(1, 6) \cong 13.5 \text{ nm}) \quad (47)$$

two transitions that occur in the range of a radii of QD (42) is added to the transition between (1, 5) and (1, 4) states, which range is in the range of QD radii

$$a_c^*(1, 5) \leq a < (a_c(1, 5) \cong 12.14 \text{ nm}) \quad (48)$$

will be interband, with photon energy

$$\Delta E_4^5(a) \cong 1.128 \text{ eV} \quad (49)$$

in the range of radii

$$a_c(1, 5) \leq a < a_c^*(1, 6) \quad (50)$$

such transition is intraband with photons energies

$$0.876 \text{ eV} < \Delta E_4^5(a) \leq 1.128 \text{ eV} \quad (51)$$

In the same range of QD radii (47) intraband transitions between the states (1, 3) and (1, 2) occurs with the photon energies

$$20 \text{ meV} \leq \Delta E_2^3(a) \leq 351 \text{ meV} \quad (52)$$

and intraband transitions between the states (1, 4) and (1, 3) is observed with photon energies

$$351 \text{ meV} \leq \Delta E_3^4(a) \leq 801 \text{ meV} \quad (53)$$

In the range a of QD

$$a_c^*(1, 6) \leq a < (a_c^*(1, 7) \cong 15.2 \text{ nm}) \quad (54)$$

there are three transitions: intraband transitions between the states of (1, 4) and (1, 3), and between (1, 5) and (1, 4) with photon energies which are in the following ranges respectively:

$$20 \text{ meV} \leq \Delta E_3^4(a) \leq 351 \text{ meV} \quad (55)$$

$$326 \text{ meV} \leq \Delta E_4^5(a) \leq 876 \text{ meV} \quad (56)$$

transitions between (1, 6) and (1, 5) in the range of QD radii

$$a_c^*(1, 6) \leq a < (a_c(1, 6) \cong 13.84 \text{ nm}) \quad (57)$$

will be intraband with the photon energy

$$\Delta E_5^6(a) \cong 1.302 \text{ eV} \quad (58)$$

and in the range of QD radii

$$a_c(1, 6) \leq a < a_c^*(1, 7) \quad (59)$$

Such transition is intraband with photon energies

$$0.901 \text{ eV} < \Delta E_5^6(a) \leq 1.302 \text{ eV} \quad (60)$$

In the range of QD a radii

$$a_c^*(1, 7) \leq a < (a_c^*(1, 8) \cong 16.8 \text{ nm}) \quad (61)$$

there are three transitions: two intraband between states (1, 5) and (1, 4), and also between the states of (1, 6) and (1, 5) with photon energies which lie in the ranges, respectively

$$0 \text{ meV} \leq \Delta E_4^5(a) \leq 326 \text{ meV} \quad (62)$$

$$876 \text{ meV} \leq \Delta E_5^6(a) \leq 901 \text{ meV} \quad (63)$$

Transition between (1, 7) and (1, 6) states in the range of QD radii

$$a_c^*(1, 7) \leq a < (a_c(1, 7) \cong 15.5 \text{ nm}) \quad (64)$$

in intraband with the photon energy

$$\Delta E_6^7(a) \cong 1.502 \text{ eV} \quad (65)$$

in the range of a

$$a_c(1, 7) \leq a < a_c^*(1, 8) \quad (66)$$

this transition will be intraband with photon energies with the range of

$$0.876 \text{ eV} < \Delta E_6^7(a) \leq 1.502 \text{ eV} \quad (67)$$

In the range of a

$$a_c^*(1, 8) \leq a < (\tilde{a}_c \cong 19.1 \text{ nm}) \quad (68)$$

there are three transitions: two intraband between states (1, 6) and (1, 5), and between the states (1, 7) \rightarrow (1, 6) with photon energies lying in the ranges respectively:

$$263 \text{ meV} \leq \Delta E_5^6(a) \leq 876 \text{ meV} \quad (69)$$

$$776 \text{ meV} \leq \Delta E_6^7(a) \leq 876 \text{ meV} \quad (70)$$

transition between (1, 8) and (1, 7) states in the range of QD

$$a_c^*(1, 8) \leq a < (a_c(1, 8) \cong 17.16 \text{ nm}) \quad (71)$$

will be intraband with photons energies

$$\Delta E_7^8(a) \cong 1.903 \text{ eV} \quad (72)$$

In the range of a

$$a_c(1, 8) \leq a \leq \tilde{a}_c \quad (73)$$

there are three intraband transitions: the transition between the states (1, 6) and (1, 5) with photons energies in the interval

$$0 \leq \Delta E_5^6(a) \leq 263 \text{ meV} \quad (74)$$

transition between (1, 7) and (1, 6) states with photon energies

$$0 \leq \Delta E_6^7(a) \leq 776 \text{ meV} \quad (75)$$

and transition between (1, 8) and (1, 7) states with photon energies

$$0 \leq \Delta E_7^8(a) \leq 1.903 \text{ eV} \quad (76)$$

Thus, in the nanosystem in which average values of aluminum oxide QD radii vary in the range of:

$$a_c^*(1, 1) \leq a \leq \tilde{a}_c \quad (77)$$

interband and intraband transitions create energy bands, lying in the QD bandgap. Energy of photons $\Delta E_i^{l+1}(a)$ (26) of such interband and intraband transitions reach high values comparable to the binding energy $E_{ex}^{2D} \cong 2.504 \text{ eV}$ (17) of the ground state of two-dimensional exciton (see Figure 1 and Table 1). Energies of the interband transitions $\Delta E_i^{l+1}(a)$ (26) are significantly exceed the energies corresponding to the intraband transitions for given average radius of QD a (in the interval (77)). Spectra of emission, absorption and transmittance of light, which are located in the visible and infrared wavelengths, are formed from such energy bands. Such spectra were observed in experimental works [2–4].

It should be noted that in the nanosystems, in which average a radii of aluminum oxide QD vary in the interval (77) at T temperature satisfying

$$\Delta E_i^{l+1}(a) \gg k_B T \quad (78)$$

(where k_B —Boltzmann constant), the observation of nanosystems is possible in the processes of absorption and emission on the transitions with frequencies $(\Delta E_i^{l+1}(a)/\hbar)$, depending on the values

of the average radius of the QD (in the interval (77)), lying in the range from the infrared to the visible spectrum. Such processes do not occur on QD with small radii $a < a_c^*(1, 1) \cong 4.9$ nm. New transition states $(1, l)$, starting from $(1, 0)$ at $a \geq a_c^*(1, 1)$ to $(1, 8)$ state at $a \geq a_c^*(1, 8)$ (see Table 1), will give a contribution to the absorption (and also emission) at large values of QD radii $a \geq a_c^*(1, l \leq 8)$. Therefore, for instance, it is possible spectroscopically control the nucleation of QD in the dielectric matrix, fixing the formation stage of the QD, starting from the radii $a \geq a_c^*(1, 1)$, i.e., the emergence of a new phase in the nanosystem. The dependence of the energy spectrum of $E_{1,l}(a)$ (22) of the exciton on the a radius of QD and its threshold feature enable opportunity to make selection by laser spectroscopy methods in nanosystems, determining the degree of dispersion of nanosystems (see Figure 1).

It should be noted that in the energy of the ground state of the exciton (22) (of spatially separated electrons and holes) in nanosystems containing aluminum oxide QD with a radii (25), the main contribution is the average value of the energy of the Coulomb interaction $\bar{V}_{eh}(a) = \langle R_l(r_e, r_h, r, a) | V_{eh}(r) | R_l(r_e, r_h, r, a) \rangle$ between the electron and hole. Wherein the average value of the energy interaction between electron and hole with her and “foreign” images gives much smaller contribution to the energy of the ground state of the exciton (22) (the ratio of which to the contribution of the average value of the Coulomb interaction energy does not exceed 8%). The latter circumstance is due to the fact that the values of the average energies of the interaction of holes and electrons with their images, as well as the values of average interaction energies of the hole and electron with “foreign” images makes contribution to the (22) with different signs, which are largely compensate each other.

Thus, the energy of the ground state of the exciton (22) (of spatially separated electrons and holes) is due to the renormalization of the Coulomb interaction energy (8) between the electron with a hole, as well as the polarization interaction energy (5) of electron and hole with spherical surface of boundary QD/matrix associated with the spatial restriction of the area of the volume quantization volume of QD.

One can see from the Figure 1, which shows the dependence of the total energy $E_{1,l}(a)$ (22) of the ground state of exciton (of spatially separated electrons and holes) in nanosystem containing aluminum oxide QD with average radius a from the interval (25), it follows that with the increase of QD radius $E_{1,l}(a)$ (19) total energy of the ground state of the exciton increases. Herewith, the energy (22) of the ground state of the exciton significantly exceeds (3–49 times) the value of the binding energy of the exciton $\tilde{E}_{ex}^{2D} \approx (-51.16$ meV) in aluminum oxide single crystal. Starting from the radius $a \geq \tilde{a}_c(1, l) = 19.1$ nm, the value of the total energy (22) of the ground state of the exciton asymptotically tends to the, accordingly, values of $E_{ex}^{2D} = (-2.5038$ eV) (17) (characterizing the binding energy of the ground state of the two-dimensional exciton (from spatially separated electrons and holes)) (see Figure 1).

3. Comparison of the Theory with Experiment

In experimental works [2–4] nanostructures containing aluminum oxide QD with small concentrations ($x = 0.03\%$), placed in the matrix (vacuum oil). At such low concentrations of QD, the interaction between the QDs can be neglected. Optical properties of such nanosystems are mainly determined by the energy spectrum of electrons and holes localized near the surface of the spherical single QDs, situated in the dielectric matrices. In [2–4] it was observed the nonlinear optical properties and their dependences on the matrix material of heterogeneous liquid nanophase composites based on wideband aluminum oxide QD with average radii not greater than $a = 25$ nm. In [2–4] it is shown that in the matrix (vacuum oil) aluminum oxide QD have a wide absorption band (from 1.4 eV to 3.7 eV) in the visible and near infrared regions.

To interpret the results of the experiments [2–4], we may assume that QDs have a spherical form. In [2–4] the average a radii of QD vary from 1 nm to 25 nm, as follows from the results of the variational calculation of the ground state energy $E_{1,l}(a)$ (22) of the exciton in nanosystem containing aluminum oxide QD, varying radii a in the range of (25), (see Figures 1 and 2 and Table 1) the band of surface

exciton states appears (consisting of the stationary states band with $E_{1,l} = E_{ex}^{2D} = 2.5038$ eV width, located in the band gap of QD, and from a band from quasi-stationary states $E^{max} = 0.526$ eV, located in the conduction band of QD. In [2–4] works it is revealed the formation of donor type additional band with (0.3–0.4) eV width inside the bandgap aluminum oxide QD at the depth (2.3 eV and 1.96 eV) from the bottom of the conduction band of the QD. Let us suppose that such a band can be described by the band of surface exciton states. Then in the nanosystem levels $E_d = -2.3$ eV and $(-1.96$ eV) correspond to the QDs with average radii: (14.0 nm, 14.9 nm, 16.1 nm, 17.0 nm, 18.1 nm) and (5 nm, 5.2 nm, 12.5 nm, 13 nm, 15.2 nm, 16.3 nm, 17.4 nm), respectively (see Figure 1), and besides the values of the radii lie in the range of average radii of QD studied in experimental conditions [2–4].

In the frequency region corresponding to the quasi-stationary and stationary states $(1, l)$ from the band of surface exciton states, the light wavelength is much larger than the dimensions of these states (about a_{ex}^{2D} (16)) (see Table 1). Therefore, the behavior of such states $(1, l)$ in the electromagnetic field can be well described by the dipole approximation [18,19]. In the case of the optical absorption of nanosystem containing aluminum oxide QD with average radii but not exceeding 20 nm, an electron is transferred from the stationary levels $(1, l)$ to the higher levels of the excited stationary states $(1, (l + 1))$ (the condition (78) is satisfied). As a result, the electron transitions to such highly excited exciton levels (particularly, transitions from the levels ($E_d = -2.3$ eV and $(-1.96$ eV)) [2–4]) excite the dipole moments of the transitions, the values of which are proportional to the a radii of QD and exceed by an order typical values for aluminum oxide single crystal [18,19]. Such mechanism of excitation of the dipole moments of transitions causes QD polarization in the field of the light wave, which creates an additional polarization of nanosystem, and as a result, the nonlinear increment to the refractive index of the nanosystem [2–4]. The increment in the range of frequencies below the resonance is positive. In the case of sufficient large length of interaction of light waves with the nanosystem the increase in the refractive index due to self-focusing of the beam can cause a waveguide channel. As a result, with an increase of the radiation intensity [2–4] “enlightenment” of nanosystem occurs.

Optical absorption of nanosystem causes the interband transitions between the levels of the surface exciton states—between stationary states lying in the bandgap of QD, and quasi-stationary states, located in the QD conduction band (see Figures 1 and 2 and Table 1). Such transitions lead to the increase of concentration of non-equilibrium electrons in the QD conduction band. In the case of scattering of electrons on the QD with large radii $a > a_c^*(1, l = 8) = 16.8$ nm the trapping of the electrons on the quasi-stationary states can occur without change in their total energy. As a result, the concentration of non-equilibrium electrons in the conduction band of QD can also increase. In [2–4] it was observed electron transition from quantum energy 4.1 eV with an additional band to the QD conduction band at the level of 0.4 eV. This level is in the area of quasi-stationary states. As it is shown in [2–4], the increase of the electron concentration in the QD conduction band induces the nonlinear increment to the refractive index of the nanosystems, which is negative. As a result, in the [2–4] the saturation of radiation intensity was experimentally observed increasing the intensity of the light wave due to the finite number of electronic levels in surface exciton states in the QD (see Figure 1).

4. Conclusions

The picture of the occurrence of the surface exciton states was described in the nanosystem. It was found that with the increase of a radius of QD, starting from the magnitude a greater than a certain critical radius of QD $a_c^*(1, l)$ quasi-stationary states initially appear, which with the increase of QD radius $a \geq a_c(1, l) > a_c^*(1, l)$ goes into the stationary state. Quasi-stationary and stationary states form a band of surface states of the exciton. In the nanosystem the stationary states of the exciton are located in the bandgap of aluminum oxide QD (below the bottom of the conduction band of QD, see Figure 2, area 1). They are bounded below by the level E_{ex}^{2D} , which is equal to the binding energy of the ground state of the two-dimensional exciton (from spatially separated electrons and holes). Quasi-stationary states of the exciton are in the conduction band of aluminum oxide QD (see Figure 2, area 2). They are bounded to the top by boundary of the $E_{1,l}^{max}(a)$, wherein $E_{1,l}^{max}(a)$ takes the significant

value comparable to the $E_{ex}^{2D} \cong 2.504$ eV. The mechanisms of the formation of intra—and interband absorption spectra (emission light) are presented in the nanosystem containing aluminum oxide QD, situated in the matrix (vacuum oil) [2–4]. It was found that in the nanosystem the spectra of interband absorption (emission) of light composed of the energy bands, which were formed by the electron transitions between quasi-stationary and stationary states, and intraband absorption spectra—of the zones, which were caused by the electron transitions between stationary states.

It was shown that the electron transitions from fixed levels ($1, l$) to the higher levels of the excited stationary ($1, (l + 1)$) states, belonging to the surface exciton states, which lie near the bottom of the conduction band in the bandgap of the QD (see Figures 1 and 2 and Table 1), can excite the dipole moments of the transitions, the values of which are proportional to the a radii of QD and are higher by an order than the typical values for aluminum oxide single crystal [18,19]. Such a mechanism of excitation of the dipole moments of transitions causes QD polarization in the field of the light wave and as a result, the nonlinear increment to the refractive index of the nanosystem. Such increment to the range of frequencies below the resonance is positive. As a result, with increasing the radiation intensity the “enlightenment” of the nanosystem was observed [2–4].

It was shown that the electron interband transitions between the levels of the surface exciton states of QD—between stationary states and quasi-stationary states (See Figures 1 and 2 and Table 1), leads to the increase of non-equilibrium concentration of the electrons in the conduction band of QD. The trapping of the electrons on the quasi-stationary states (without changing the total energy) of the QD with large radii $a > a_c^*$ ($1, l = 8$) = 16.8 nm also increases the concentration of non-equilibrium electrons in the conduction band of QD. Such an increase in the concentration of the electrons in the conduction band of QD is the nonlinear increment to the refractive index nanosystems [2–4], which is negative. The finite number of electronic levels in surface exciton states of QD (see Figure 1) leads to the increase of the light wave intensity to the saturation of the intensity of radiation observed experimentally in [2–4]. It was found that the electron transitions in the surface exciton states caused significant absorption of the radiation in the visible and near-infrared wavelengths and occurred blurring of the experimentally observed absorption edges [2–4].

Author Contributions: All authors have done theoretical calculations; Sergey I. Pokutnyi, Yu. N. Kulchin, Vladimir P. Dzyuba and David B. Hayrapetyan analyzed the obtained results and wrote the paper. Sergey I. Pokutnyi edited and submitted the paper.

Conflicts of Interest: The authors declare no conflict of interest.

References

- Grabovskis, V.J.; Dzenis, Y.Y.; Ekimov, A.I. Photoionization of semiconductor microcrystals in glass. *Sov. Phys. Solid State* **1989**, *31*, 272–275.
- Kulchin, Y.N.; Shcherbakov, A.V.; Dzyuba, V.P. Nonlinear-optical properties of heterogeneous liquid nanophase composites based on high-energy-gap nanoparticles. *Quantum Electron.* **2008**, *38*, 154–158. [[CrossRef](#)]
- Dzyuba, V.P.; Kulchin, Y.N.; Milichko, V.A. Nonlinear refractive index of dielectric nanocomposites in weak optical fields. *Tech. Phys. Lett.* **2010**, *36*, 973–977. [[CrossRef](#)]
- Dzyuba, V.P.; Kulchin, Y.N.; Milichko, V.A. Quantum size states of a particle inside the nanospheres. *Adv. Mater. Res. A* **2013**, *677*, 42–48. [[CrossRef](#)]
- Pokutnyi, S.I. On an exciton with a spatially separated electron and hole in quasi-zero-dimensional semiconductor nanosystems. *Semiconductors* **2013**, *47*, 791–798. [[CrossRef](#)]
- Pokutnyi, S.I.; Kulchin, Y.N.; Dzyuba, V.P. Binding energy of excitons formed from spatially separated electrons and holes in insulating quantum dots. *Semiconductors* **2015**, *49*, 1311–1315. [[CrossRef](#)]
- Efros, A.L. Interband absorption of light in a semiconductor sphere. *Sov. Phys. Semicond.* **1982**, *16*, 772–775.
- Pokutnyi, S.I.; Kulchin, Y.N.; Dzyuba, V.P.; Amosov, A.V. Biexciton in nanoheterostructures of dielectric quantum dots. *J. Nanophotonics* **2016**, *10*, 036008. [[CrossRef](#)]
- Kaftelen, H.; Ocakoglu, K.; Thomann, R.; Tu, S.; Weber, S.; Erdem, E. EPR and photoluminescence spectroscopy studies on the defect structure of ZnO nanocrystals. *Phys. Rev. B* **2012**, *86*, 014113. [[CrossRef](#)]

10. Bansal, A.K.; Antolini, F.; Zhang, S.; Stroea, L.; Ortolani, L.; Lanzi, M.; Serra, E.; Allard, S.; Scherf, U.; Samuel, I.D.W. Highly luminescent colloidal CdS quantum dots with efficient near-infrared electroluminescence in light-emitting diodes. *J. Phys. Chem. C* **2016**, *120*, 1871–1880. [[CrossRef](#)]
11. Repp, S.; Erdem, E. Controlling the exciton energy of zinc oxide (ZnO) quantum dots by changing the confinement conditions. *Spectrochim. Acta Part A* **2016**, *152*, 637–644. [[CrossRef](#)] [[PubMed](#)]
12. Li, C.; Jiang, D.; Zhang, L.; Xia, J.; Li, Q. Controlled synthesis of ZnS quantum dots and ZnS quantum flakes with graphene as a template. *Langmuir* **2012**, *28*, 9729–9734. [[CrossRef](#)] [[PubMed](#)]
13. Daumann, S.; Andrzejewski, D.; Di Marcantonio, M.; Hagemann, U.; Wepfer, S.; Vollkommer, F.; Bacher, G.; Epple, M.; Nannen, E. Water-free synthesis of ZnO quantum dots for application as an electron injection layer in light-emitting electrochemical cells. *J. Mater. Chem. C* **2017**, *5*, 2344–2351. [[CrossRef](#)]
14. Lozovik, Y.E.; Nishanov, V.N. Exciton Wannier-Mott near the interface. *Sov. Phys. Solid State* **1976**, *18*, 1905–1911.
15. Efremov, N.A.; Pokutnyi, S.I. Spectrum of local states of charge carriers in the ultradisperse media. *Sov. Phys. Solid State* **1990**, *32*, 1697–1706.
16. Efremov, N.A.; Pokutnyi, S.I. The broadening of the quasi-stationary states of carriers in ultradisperse media. *Sov. Phys. Solid State* **1991**, *33*, 1607–1612.
17. Pokutnyi, S.I. Size quantization of the exciton in quasi-zero-dimensional structures: Theory. *Phys. Lett. A* **1995**, *203*, 388–394. [[CrossRef](#)]
18. Pokutnyi, S.I. Absorption and scattering of light in quasi-zero-dimensional structures: II. Absorption and scattering of light by single-particle local states of the charge carriers. *Sov. Phys. Solid State* **1997**, *39*, 528–532. [[CrossRef](#)]
19. Pokutnyi, S.I. Absorption and scattering of light in quasi-zero-dimensional structures: I. Transition dipole moments of the carriers. *Sov. Phys. Solid State* **1997**, *39*, 634–636. [[CrossRef](#)]



© 2018 by the authors. Licensee MDPI, Basel, Switzerland. This article is an open access article distributed under the terms and conditions of the Creative Commons Attribution (CC BY) license (<http://creativecommons.org/licenses/by/4.0/>).